Available online at www.sciencedirect.com

ScienceDirect

Procedia Chemistry 15 (2015) 33 – 41

Procedia Chemistry

16th International Scientific Conference "Chemistry and Chemical Engineering in XXI century" dedicated to Professor L.P. Kulyov, CCE 2015

CO_2 sequestration by natural zeolite for greenhouse effect control

Miguel Angel Hernandez[a], Alexey Pestryakov[b], Roberto Portillo[c], Martha A. Salgado[c], Fernando Rojas[d], Efrain Rubio[e], Sinuhe Ruiz[f], Vitalii Petranovskii[g,*]

[a]*Departamento de Investigacion en Zeolitas, BUAP, Puebla, Mexico*
[b]*Tomsk Polytechnic University, Tomsk 634050, Russia*
[c]*Facultad de Ciencias Químicas, Universidad Autónoma de Puebla, México*
[d]*Departamento de Química, Universidad Autónoma Metropolitana-Iztapalapa, Apartado Postal 55-534, México 09340, D.F.*
[e]*Centro Universitario de Vinculación y Transferencia de Tecnología, Universidad Autónoma de Puebla*
[f]*Facultad de Ingeniería Química, Universidad Autónoma de Puebla, México*
[g]*Centro de Nanociencias y Nanotecnología, Universidad Nacional Autonoma de Mexico, Carretera Tijuana-Ensenada, Km. 107, Ensenada, B.C. Mexico; On the sabbatical leave at: Departamento de Investigación en Zeolitas, Instituto de Ciencias BUAP, Puebla 72570, México*

Abstract

This paper describes the adsorption of CO_2 on pores in natural erionite exchanged with aqueous solutions of Na^+, Mg^{2+}, and Ca^{2+} salts at different concentrations, variable time and temperature of treatment. Experimental data of CO_2 adsorption were treated by the Freundlich and Langmuir equations. Complementarily were evaluated standard adsorption energies and the degree of interaction of the gas with the zeolite; the evolution of isosteric heats of adsorption was analyzed. The exchange with Na^+ favors the creation of emergent pores thus causing an increase of the adsorption capacity for CO_2. The presence of Na^+ at micropore entrances causes an increased adsorption into the nanocavities and on the external area of the ion-exchanged zeolites. The development of nanopores in erionite was evaluated through the Barrett-Joyner-Halenda and NLDFT methods. Depending on the conditions of the exchange treatment, Na^+ was found to be most favorable, well distributed, and accessible for N_2 adsorption.

Peer-review under responsibility of Tomsk Polytechnic University

Keywords: sequestration ; carbon dioxide ; erionite ; adsorption

* Corresponding author. Tel.: +52-(646)-175-0650; fax: +52-(646)-174-4603.
E-mail address: vitalii@cnyn.unam.mx

Peer-review under responsibility of Tomsk Polytechnic University
doi:10.1016/j.proche.2015.10.006

1. Introduction

Carbon dioxide (CO_2) has become an important global issue due to the gradual increase in the atmospheric concentration of CO_2 resulted from fossil fuel combustion and the link between an increase in the CO_2 concentration in the atmosphere and global climate changes. Therefore, it is necessary to reduce CO_2 concentration significantly from the current level[1]. Up to now, various technologies, such as amine solutions for absorption, membrane separation and adsorption-based separation were employed to stabilize the CO_2 concentration in the atmosphere by controlling the emission of CO_2 from various sources[2-4]. Adsorption, in fact, has become the state of the art technology for the separation and recovery of CO_2 [5]. Although the conventional sorbents such as activated carbons and zeolites possess relatively high CO_2 adsorption capacities at room temperature, the adsorbed amounts of CO_2 on these adsorbents will decline rapidly with increasing temperature. Additionally, the adsorption selectivity for CO_2 on activated carbons and zeolites in the presence of water vapor will become very poor[6]. At high temperatures, hydrotalcites can adsorb CO_2, but their adsorption capacities towards CO_2 are, in general, low. Basic metal oxides such as MgO and CaO have extremely large absorption capacities for CO_2 but the regeneration of these absorbents is performed at higher temperatures, resulting in severe energy penalties[7]. Therefore, the development of efficient adsorbents is of utmost importance for CO_2 capture and separation. Among the suggested materials for adsorption of CO_2 bests itself are zeolites of ERI type, outstanding by their high adsorption capacity, accessibility, purity and, especially, by possibility to increase their adsorption capacity by incorporating certain cations through ion exchange, and via nanodeposits formation in the internal structure of this zeolite. The replacement by ion exchange of Na^+ ions in natural erionite by either Ca^{2+} or H^+ ions increases the capacity (i.e. the accessible pore volume). Ion exchange (via a salt) and dealumination (with acid treatments) of erionite lead to the formation of a secondary porosity (i.e., mesopores are created)[8]. The cavities in erionite after an ion exchange process can accommodate metal ions and clusters produced by a subsequent reduction reaction[9-10]. Cation type and location of water molecules within the zeolite structure are still under investigation[11]. The objectives of this study are to compare the experimental results for CO_2 adsorption obtained by the dynamic method in erionite zeolites exchanged with Na^+, Ca^{2+} and Mg^{2+} to determine the order of selectivity with respect to this gas in the zeolites studied. With this purpose in mind, CO_2 adsorption isotherms on microporous ERI solids at different temperatures were measured through the gas chromatographic (GC) peak maxima technique[12]. In this paper, we are also reporting isosteric heats of adsorption evaluated at different CO_2 loadings. Finally, we examine sorption capacities and isosteric heats of adsorption in terms of the structural properties of our assortment of ERI zeolites. To follow, for this study were used methods of X-ray diffraction (XRD), scanning electron microscopy (SEM), Energy Dispersive Spectroscopy (EDS), High Resolution Adsorption Studies (HRADS), and gas chromatography.

2. Experimental Section

Mexican natural zeolites proceeding from Agua Prieta in the State of Sonora, Mexico were used in this work. The ERIN label accounts for the natural erionite sample, which is free of any treatment. Exchanged erionite samples $ERICa^X$, $ERIMg^X$, and $ERINa^X$ were prepared from ERIN precursor and exchanged either X=1, X=2, or X=3 times with 0.1 N solutions of the corresponding cation chloride salts (i.e. $CaCl_2$, $MgCl_2$, NaCl) at 50 °C for 6 h. N_2 and He ultrahigh purity gases (> 99.999%, INFRA Corp.) were employed for the textural sorption studies of natural and exchanged erionites.

XRD patterns were determined by means of a Siemens D-500 diffractometer employing a nickel filtered Cu K_α radiation and compared with the corresponding JCCPD files for identifying the phases presented in the erionite samples. Scanning Electron Microscopy images were obtained from a Vega Tescan, model JSM-5300 electron microscope equipped with an energy dispersive spectrometer (EDS) probe, which allows a semiquantitative determination of local composition at the nanoscale level. All N_2 adsorption isotherms were measured at the boiling point of liquid N_2 (76.4 K at the 2200 m altitude of Puebla City, México) in an automatic volumetric adsorption system (Quantachrome AutoSorb-1LC). N_2 adsorption isotherms were determined in the interval of relative pressures, p/p^0, extending from 10^{-5} to 0.995. The saturation pressure, p^0, was continuously registered in the course of the adsorption-desorption measurements. Powder with particle sizes corresponding to 60-80 mesh were sampled

from all specimens under analysis. Prior to the sorption experiments, samples were outgassed at 623 K during 20 h at a pressure lesser than 10^{-6} mbar.

Experiments on CO_2 adsorption over substrates were performed on a gas chromatograph Gow-Mac 350 equipped with a thermal conductivity detector. Chromatographic columns are stainless steel (with internal diameter of 5 mm and length of 50 cm) and were packed with zeolite granules equivalent to mesh sizes 0.250 mm. Prior to adsorption of the gas, each sample was pretreated in situ under flowing He at 573 K. Subsequently, various volumes of CO_2 were injected into the column to measure the retention time. The adsorption isotherms of the gas on the zeolites are measured at various temperatures (463, 493, 523, 553 and 583 K); assessments of adsorbed amount function of pressure are effected applying the method of maximum chromatographic peaks (GC peak maxima method) using helium (30 cm^3min^{-1}) as carrier gas. The isosteric heat of adsorption at low degrees of coverage was calculated from the experimental adsorption isotherm data using the Clausius-Clapeyron equation.

Data corresponding to the adsorption of CO_2 on erionite samples were fitted to standard Freundlich isotherm models through linear regression in order to determine the adsorption parameters pertinent to each of the above approaches. The Freundlich adsorption equation can be written as:

$$a = K_F + p^{1/n} \quad (1)$$

where a is the adsorbed amount (mmol g^{-1}), K_F is the Freundlich adsorption constant, and n is an exponential factor.

All CO_2 adsorption data were fitted to standard Langmuir adsorption equation through linear regression. From gas adsorption data at low pressures, it is possible to evaluate the Henry constants (K_H) at different temperatures for the series of adsorbent-adsorptive pairs employed in this work according to the following expression[13]:

$$K_H = lim_{p \to 0} (a/a_m p) \quad (2)$$

where a represents the amount adsorbed on the solid walls at pressure p, while a_m is the monolayer capacity evaluated from the Langmuir equation:

$$\theta = a/a_m = Kp/1+Kp \quad (3)$$

where $K\,a_m = K_H$ is, something that can be tested graphically by plotting $1/a$ versus $1/p$:

$$1/a = 1/a_m + 1/a_m Kp \quad (4)$$

Standard adsorption energies ($-\Delta U_0$) can be found from the temperature dependence of Henry constants K_H (at low pressures $K_H \approx K_F$), a relationship that is assumed to be consistent with a traditional van't Hoff form:

$$(\partial \ln K_H/\partial T) = \Delta U_0/ RT^2;\ K_H = K_0\, exp\_(-\Delta U_0/ RT) \quad (5)$$

where $\Delta U_0 = \Delta H_0 + RT$; ΔH_0 is the standard adsorption enthalpy, R the universal gas constant, and K_0 is van't Hoff's pre-exponential factor.

The isosteric heat of adsorption, q_{st} (kcal mol^{-1}), at different adsorbate loadings can be evaluated from the adsorption isotherms data through a Clausius-Clapeyron type equation[14]:

$$[\partial \ln p /\partial T]_a = q_{st}\, a/RT^2 \quad (6)$$

where p and T are the equilibrium pressure and temperature at a given adsorbate loading (a).

3. Results and discussion

The texture properties and chemical composition of the zeolites are reported in Tables 1 and 2. The results of texture (A_{SB}, BET specific surface area; A_{SL}, Langmuir specific surface area; A_{St}, t-plot surface area; C_B, BET

constant; V_{Σ}, volume adsorbed at $p/p^0 = 0.95$ and expressed as the volume of liquid N_2 (Gurvitch rule); W_0, volume micropore estimated from *t*-plots, and $V_{meso} = V_{\Sigma} - W_0$, and mesopore volume) are listed in Table 1. The interesting features of ion-exchanged zeolites are their large surface area and micropore volume. Additionally it is observed that the BET constant values (C_B) are negative, thus indicating the inadequacy of the micropore filling mechanism given the continuous growth of the adsorbed layer on the surface of these substrates[15]. The behavior of the textural parameters of natural and exchanged erionites obey the following sequence: A_{SL}: ERINa: 3>2>1; ERICa: 2>1>3; ERIMg: 2>1>3. While V_{Σ}: ERINa: 3>2>1; ERICa: 2>1>3; ERIMg: 2>1>3. Finally, W_{0t}: ERINa: 3>2=1, ERICa: 2>1>3, and ERIMg: 2>1>3. There exists an almost total concordance between the tendencies of the A_{SL}, V_{Σ} and W_{0t}. The EDS chemical compositions of all erionite substrates are listed in Table 2. This Table reveals that the amount of cation present in each zeolite increased, once the corresponding ion exchange has been carried out.

The dynamic chromatographic method was used for evaluating the adsorption isotherms from injection pulse data proceeding from the elution curves of the adsorptives on the zeolites under study. These CO_2 adsorption isotherms were measured in a region of low adsorbate concentrations; hence, adsorption on the mesopore surface can be practically neglected. Consequently, the parameters that characterize the microporous structure of our erionite adsorbents have been calculated from the CO_2 adsorption isotherms, without introducing any correction for adsorption on the mesopore surface. CO_2 adsorption isotherms at different temperatures on ERIN and ERINa zeolites are presented in parts a-d of Figure 1, while the isotherms of ERICa and ERIMg zeolites are presented in parts a-f of Figure 2. Complementarily were evaluated standard adsorption energies $-\Delta U_0$ while the degree of interaction of the gas with the zeolite was analyzed by the evolution of isosteric heats of adsorption $-q_{st}$. Values of Freundlich constants K_F and n, Henry constants K_H, Langmuir monolayer capacity a_m, adsorption energies $-\Delta U_0$ and isosteric heat of adsorption $-q_{st}$ are given in Table 3. From this Table it is established that the highest values purchase for the monolayer capacity at 473 K is obtained by the sample ERICa2, while lower values acquires the sample ERIMg3. On the other hand, treatments with NaCl at different contact times and concentrations produce increases in adsorptivity, proving to be ERINa2 most favored adsorbent, see Table 2.

The Langmuir approach works reasonably well for all but one case: that corresponding to adsorption at 588 K on ERINa1, ERICa3 and ERIMg3. Similar behaviors are presented in ERINa2 at 623 K and ERICa2 at 503 K. The values of the Henry and Langmuir constants (i.e., K_H and a_m) are listed in Table 3. The temperature dependence of the monolayer adsorption capacity (a_m), derived from the Langmuir plots, have the lowest values in ERIMg3 and ERIMg2 zeolites; on the contrary the highest values correspond to ERINa2 and ERINa3 zeolites.

The Freundlich model can be fitted extremely well to most CO_2 adsorption data, although is not suitable for ERICa1and ERICa3 at 473, 503 and 534 K, or for ERINa2 and ERIMg2 at 473 K. The values of the Freundlich parameters (K_f and n) related to CO_2 adsorption on ERI zeolites are listed in Table 3.

Table 1. Textural parameters of natural (ERIN) and ion-exchanged (Na^+, Ca^{2+}, and Mg^{2+}) erionite zeolites as determined from N_2 adsorption.

ERI	A_{SL} m^2/g	A_{SB} m^2/g	A_{St} m^2/g	C_B	V_{Σ} cm^3/g	W_{0t} cm^3/g	V_{meso} cm^3/g
ERIN	243.9	169.22	12.99	-70	0.101	0.076	0.025
ERINa1	244.7	205.4	11.91	-493	0.101	0.145	0.044
ERINa2	504.4	389.6	21.08	-581	0.189	0.145	0.044
ERINa3	545.7	416.7	15.33	-260	0.205	0.16	0.045
ERICa1	325.5	270.6	29.65	-165	0.157	0.102	0.055
ERINCa2	331.5	292.1	30.68	-564	0.162	0.106	0.056
ERICa3	293.8	255.9	31.35	-628	0.147	0.089	0.058
ERIMg1	322.7	289.0	30.97	-689	0.159	0.104	0.055
ERIMg2	343.8	304.6	33.85	-571	0.169	0.109	0.060
ERIMg3	309.4	275.9	24.14	-653	0.148	0.100	0.048

Table 2. Chemical composition (mass %) of erionites as determined by EDS.

	ERIN	Na1	Na2	Na3	Ca1	Ca2	Ca3	Mg1	Mg2	Mg3
NaO	3.694	3.986	4.42	4.103	2.670	2.110	1.551	3.357	3.339	2.836
MgO	1.194	1.536	1.376	1.453	1.719	1.702	1.685	2.122	2.155	2.365
Al_2O_3	11.21	13.34	14.02	14.08	13.01	13.18	13.36	13.66	13.66	13.13
SiO_2	54.85	57.65	56.13	60.01	57.66	57.43	57.21	59.05	60.17	59.36
K_2O	2.309	1.939	1.670	1.879	2.718	2.648	2.578	2.718	2.650	2.763
CaO	1.222	1.315	1.502	1.810	1.814	2.507	3.200	1.250	1.101	1.035
Fe_2O_3	1.801	2.373	0.605	0.682	3.031	2.962	2.893	2.755	3.103	2.407
FeO	1.621	2.136	0.545	0.613	2.727	2.665	2.603	2.479	2.792	2.166
Si/Al	4.893	4.320	4.004	4.261	4.429	4.356	4.283	4.321	4.405	4.518

Table 3. Henry, Freundlich and Langmuir parameters for the adsorption of CO_2 on ERIN and ERI exchanged zeolites.

Sample	T, K	K_H x 10^2 mmol g^{-1} $mmHg^{-1}$	a_m, mmol g^{-1}	R_L	K_f x10^2 mmol g^{-1} $mmHg^{-1}$	n	R_f
	473	2.069	0.155	0.996	2.125	1.636	0.988
	503	1.531	0.160	0.996	1.759	1.602	0.990
ERINAT	543	0.859	0.179	0.998	1.188	1.528	0.990
	588	0.713	0.173	0.996	1.088	1.579	0.993
	623	0.615	0.165	0.992	0.929	1.537	0.995
	473	3.617	0.238	0.998	3.581	1.616	0.991
	503	2.856	0.216	0.997	2.994	1.630	0.992
ERINa1	543	1.689	0.236	0.996	2.014	1.511	0.995
	588	1.571	0.186	0.980	1.900	1.631	0.998
	623	1.060	0.216	0.994	1.395	1.495	0.995
	473	5.171	0.206	0.999	4.641	1.844	0.986
	503	2.679	0.238	0.999	2.963	1.509	0.988
ERINa2	543	2.131	0.191	0.990	2.468	1.700	0.996
	588	1.400	0.242	0.998	1.723	1.460	0.994
	623	1.070	0.201	0.985	1.383	1.516	0.998
	473	5.759	0.211	0.996	4.777	1.768	0.990
	503	2.887	0.255	0.998	2.963	1.509	0.991
ERINa3	543	2.282	0.218	0.996	2.543	1.610	0.992
	588	1.739	0.220	0.996	2.005	1.535	0.998
	623	1.292	0.247	0.988	1.607	1.454	0.996
	473	1.902	0.148	0.995	2.067	1.717	0.986
	503	1.325	0.168	0.995	1.620	1.587	0.986
ERICa1	543	0.939	0.166	0.998	1.282	1.580	0.987
	588	0.816	0.163	0.993	1.197	1.617	0.995
	623	0.636	0.179	0.996	0.982	1.542	0.994
	473	2.300	0.274	0.988	2.914	1.690	0.996
ERICa2	503	1.839	0.272	0.983	2.602	1.720	0.996
	543	0.993	0.303	0.987	1.660	1.591	0.997

	588	0.902	0.317	0.988	1.471	1.524	0.999
	623	0.649	0.361	0.996	1.029	1.396	0.996
ERICa3	473	2.261	0.134	0.999	2.365	1.852	0.976
	503	1.848	0.130	0.997	2.087	1.857	0.983
	543	1.528	0.127	0.993	1.851	1.848	0.987
	588	1.438	0.117	0.981	1.921	2.063	0.995
	623	1.239	0.125	0.985	1.635	1.854	0.995
ERIMg1	473	1.549	0.140	0.996	1.691	1.614	0.990
	503	1.126	0.145	0.995	1.338	1.548	0.991
	543	0.740	0.160	0.996	0.996	1.487	0.991
	588	0.609	0.136	0.987	0.907	1.587	0.998
	623	0.549	0.136	0.984	0.886	1.632	0.996
ERIMg2	473	2.379	0.136	0.999	2.260	1.653	0.972
	503	2.445	0.110	0.991	2.328	1.961	0.985
	543	1.280	0.119	0.998	1.596	1.809	0.979
	588	1.110	0.119	0.993	1.530	1.852	0.988
	623	0.915	0.111	0.991	1.265	1.787	0.993
ERIMg3	473	1.436	0.090	0.985	1.465	1.789	0.992
	503	1.000	0.093	0.987	1.205	1.772	0.993
	543	0.882	0.093	0.988	1.143	1.797	0.995
	588	0.900	0.086	0.982	1.267	2.020	0.992
	623	0.821	0.088	0.979	1.241	2.052	0.993

The trends of the isosteric heat of adsorption (q_{st}) as a function of the amount of adsorbed CO_2 on ERI zeolites are presented in Table 4. Sorption data of CO_2 on some other adsorbents that were previously studied[16-18] are reported for comparison. The q_{st} values related to the ERI substrate corresponds to the following sequence: ERIN; ERINa2 > ERINa3 > ERINa1; ERICa2 > ERICa1 > ERICa3; ERIMg2 > ERIMg1 > ERIMg3. The enrichment of structure by Na^+ ensures the participation of these cations in the interaction with CO_2 quadrupole (0.64 A^3) generating an improved adsorption centers (Table 4). These results can be explained considering the difference in the physical and chemical properties of CO_2 molecule. First, its critical diameter is equal to 0.31 nm, with the polarizability equal to 1.9 A^3 [19]. This effect makes that the molecule is influenced to a greater extent by the electric field, which create the cations presented in solid. It is very likely that differences in properties of this gas are responsible for the CO_2 to be adsorbed in remote sites, as this molecule interacts specifically with the electric field of solid. Therefore, because the q_{st} values proceeding from CO_2 adsorption on ERIN, ERINa1, ERINa2, ERINa3 and ERICa2 are larger than the enthalpies of vaporization (17.165 kJ mol^{-1}), the adsorptive molecules interact strongly both with the surface and with the neighboring adsorbate molecules[20]. Hence, the primary and secondary micropore mechanism fillings seem to take place during the CO_2 adsorption on ERI samples: first, a strong interaction between adsorbate molecules and the adsorbent surface occurs; next, a cohesive interaction between adsorbate molecules is developed. The fact that the magnitudes of the isosteric heats of adsorption are different from one adsorbent to another can be related to the high interaction energy depicted by the quadrupole moment of CO_2 toward the oxygen atoms of the zeolites, cation clusters and also to the molecular sieve effect displayed by each adsorbent. The isosteric heat of adsorption of CO_2 on ERIN, ERINa1, ERINa2, ERINa3, ERICa1 and ERICa2 is associated with nearly uniform surfaces ever since the adsorption on these substrates is smaller than that taking place on ERINa2. This behavior can be attributed to the slow diffusion of the CO_2 inside the zeolitic structure mainly because of the partial blocking of pore entrances by the cations and also by the residual material that remains at the entrances of cavities. According to this, it can be expected that the available adsorption space and the different sizes of the entrance windows play major roles in the magnitudes of the isosteric

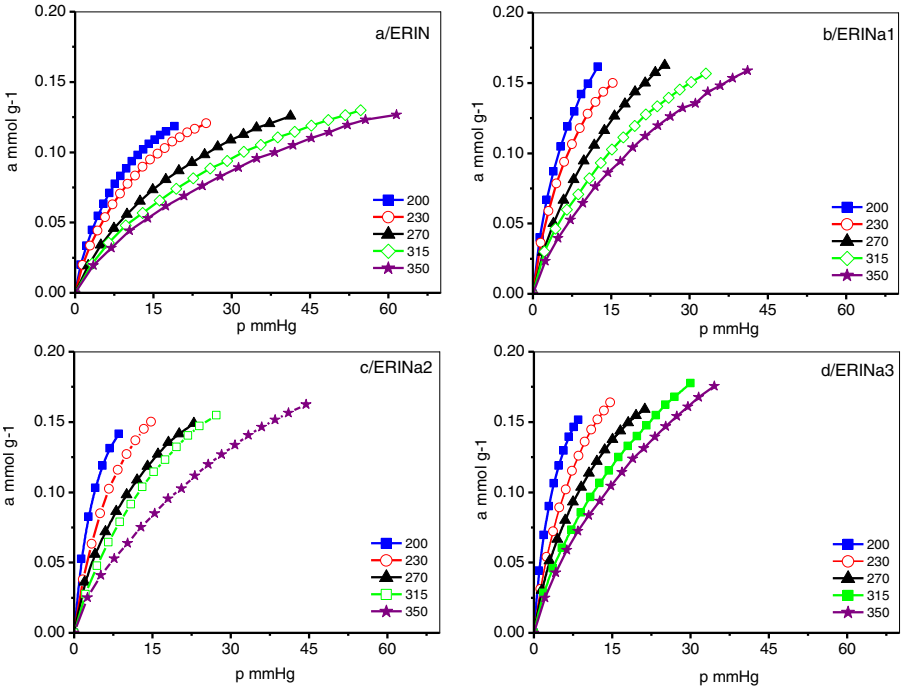

Fig. 1. Adsorption isotherms of CO_2 on ERIN and ERINa zeolites.

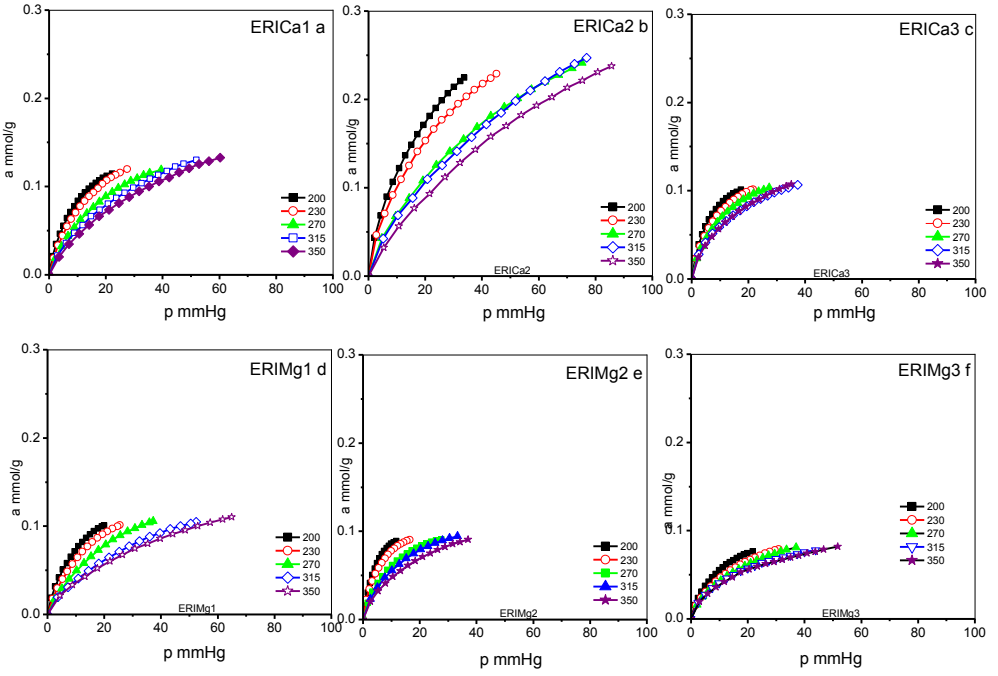

Fig. 2. Adsorption isotherms of CO_2 on ERICa and ERIMg zeolites.

Table 4. Standard adsorption energy ($-\Delta U_0$, kJ mol^{-1}) and isosteric heats of adsorption ($-q_{st}$, kJ mol^{-1}) of CO_2.

	$-\Delta U_0$	$-q_{st}$	ΔH_N
ERIN	20.471	18.800	1.634
ERINa1	19.363	21.105	3.939
ERINa2	24.155	26.285	9.119
ERINa3	22.205	22.355	5.189
ERICa1	17.079	15.659	
ERICa2	20.725	16.823	-0.33
ERICa3	9.233	10.557	-6.69
ERIMg1	17.246	17.612	0.446
ERIMg2	17.320	18.584	1.418
ERIMg3	7.859	10.557	-6.09
Silicalite		20	
13X		40	
SBA-15		30	

heats of CO_2 adsorption on ERIN and ERINa2. Therefore, progressive Na-exchange treatment of ERI develops into wider and wider pore entrances by cation exchange and larger and larger micropore volumes; so these two effects allow an increased adsorption and a cohesive interaction between adsorbed molecules. Based on the two latter effects, progressive Na exchange treatment of ERI ensures the participation of a greater number of adsorption centers in exchanged zeolites. Another possible effect produced by exchange treatment is the transformation of ultramicropore entities into supermicropore cavities, in which secondary (cohesive) adsorption is likely to take place.

4. Conclusions

Ion exchange treatments via Na^+, Ca^{2+}, and Mg^{2+} salts of natural high-silica erionites can render efficient nanoporous substrates for the adsorption of different compounds. Either protons or smaller ionic species can substitute large blocking cations at the pore entrances of natural erionite, facilitating access of different molecules into the channels of erionite. The concomitant modified structure created by the ion-exchange treatment enhances the microporous channel widths, thus creating supermicropore structures. The changes experienced by the nanoporosity of natural and exchanged erionite are conveniently described by the Dubinin-Astakhov approach since the calculated values match the amplitudes of the cavities of this zeolite. Mesoporosity caused by the ion exchange treatment can be approximately evaluated via the BJH method. The highest adsorption capacity of these erionite zeolites is presented when ERIN is ion-exchanged with Na^+.

Acknowledgements

This work was supported by the VIEP and CUVyTT, the Academic Body "Investigación en zeolitas", CA-95 (PROMEP-SEP). The authors acknowledge funding for this research by the Russian Government Program «Science» of Tomsk Polytechnic University, grant No. 4.1187.2014/K, and by UNAM-PAPIIT, Mexico, through the grant IN110713. V. Petranovskii thankful to DGAPA-UNAM for support of his sabbatical stay in BUAP.

References

1. Yang J, Zhao Q, Xu H, Li L, Dong J, Li J. Adsorption of CO_2, CH_4, and N_2 on gas diameter grade ion-exchange small pore zeolites. *J Chem Eng Data* 2012;**57**:3701-9.
2. Maurin G, Belmabkhout Y, Pirngruber G, Gaberova L, Llewellyn P. CO_2 adsorption in LiY and NaY at high temperature: molecular simulations compared to experiments. *Adsorption* 2007;**13**:453-60.

3. Belmabkhout Y, Sayari A. Effect of pore expansion and amine functionalization of mesoporous silica on CO_2 adsorption over a wide range of conditions. *Adsorption* 2009;**15**:318-28.
4. Garcés SI, Villarroel-Rocha J, Sapag K, Korili SA, Gil A. Comparative study of the adsorption equilibrium of CO_2 on microporous commercial materials at low pressures. *Ind Eng Chem Res* 2013;**52**:6785-93.
5. Jing Y, Wei L, Wanga Y, Yu Y. Synthesis, characterization and CO_2 capture of mesoporous SBA-15 adsorbents functionalized with melamine-based and acrylate-based amine dendrimers. *Micropor Mesopor Mater* 2014;**183**:124-33.
6. Palomino M, Corma A, Rey F, Valencia S. New Insights on CO_2–Methane separation using LTA zeolites with different Si/Al ratios and a first comparison with MOFs. *Langmuir* 2010;**26**:1910-7.
7. Cheung O, Bacsik Z, Krokidas P, Mace A, Laaksonen A, Hedin F. K^+ exchanged zeolite ZK-4 as a highly selective sorbent for CO_2. *Langmuir* 2014;**30**:9682-90.
8. Hernández MA, Rojas F, Portillo R, Salgado MA, Rubio E, Sánchez A, Ruiz S. Creating Nanoporosity in Na, Ca and Mg Exchanged Erionite Zeolite. *Intern J Nanotechnol* 2015; in print.
9. Prakash AM, Larry K. Cupric ion location and adsorbate interactions in Cu(II) exchanged erionite-like SAPO-17 molecular sieve. *Langmuir* 1997;**13**:5341-8.
10. Heck RH, Chen NY. Conversion of light naphthas over sulfided nickel erionite. *Ind Eng Chem Res* 1993;**32**:1003-6.
11. Rivas FC, Petranovskii V, Ulloa RZ. Growth of copper nanoparticles in erionite matrix. *Rev Mex Fis* 2010;**56**:328-33.
12. Canet X, Nokerman J, Frere M. Determination of the Henry constant for zeolite-VOC systems using massic and chromatographic adsorption data. *Adsorption* 2005;**11**:213-6.
13. Ruthven DM, Kaul BK. Adsorption of aromatic hydrocarbons in NaX zeolite. 1. Equilibrium. *Ind Eng Chem Res* 1993;**32**:2047-52.
14. Tumsek F, Inel O. Evaluation of the thermodynamic parameters for the adsorption of some *n*-alkanes on *A* type zeolite crystals by inverse gas chromatography. *Chem Engineer J* 2003;**94**:57-66.
15. Groen JC, Peffer LA, Ramirez JP. Pore size determination in modified micro- and mesoporous materials. Pitfalls and limitations in gas adsorption data analysis. *Micropor Mesopor Mater* 2003:**60**:1-17.
16. Lee JS, Kim JH, Kim JT, Suh JK, Lee JM, Lee CH. Adsorption equilibria of CO_2 on zeolite 13X and zeolite X/Activated carbon composite. *J Chem Eng Data* 2002;**47**:1237-42.
17. Siklova H, Cejka J, Zelenak A. Amine-functionalized SBA-15 silica for the adsorption of CO_2. In: Sayari A, Jaroniec M, editors. *Nanoporous Materials*. New Jersey: World Scientific; 2008. P. 625-32.
18. Hernández MA, Portillo R, Salgado MA, Rojas F, Petranovskii V, Salas R, Pérez G. Comparación de la capacidad de adsorción de CO_2 en clinoptilolitas naturales y tratadas químicamente. *Superf Vacío* 2010;**23**:67-72.
19. Sing KSW. Characterization of porous materials: past, present and future. *Coll Surf* 2004;**241**:3-7.
20. Breck DW. *Zeolite Molecular Sieves*. New York: Wiley–Interscience; 1974; pp 644-652.